

1 **GIS-Based DRASTIC and Composite DRASTIC Indices for Assessing Groundwater**
2 **Vulnerability in the Baghin Aquifer, Kerman, Iran**

3 Mohammad Malakootian¹, Majid Nozari^{2,*}

4 Manuscript Authors details:

5 1. Mohammad Malakootian, Department of Environmental Health, School of Public Health,

6 Kerman University of Medical Sciences, Iran. E-mail: m.malakootian@yahoo.com.

7 <https://orcid.org/0000-0002-4051-6242>.

8 2. Majid Nozari, Department of Environmental Health, School of Public Health, Kerman

9 University of Medical Sciences, Iran. Tel: 98-9383921819, E-mail: nozari.m@kmu.ac.ir.

10 <https://orcid.org/0000-0003-2319-1930>.

11 **ABSTRACT**

12 The present study estimated the Kerman–Baghin aquifer vulnerability using DRASTIC and
13 composite DRASTIC (CDRASTIC) indices with the aid of geographic information system (GIS)
14 techniques. Factors affecting the transfer of contamination, including water table depth, soil media,
15 aquifer media, the impact of the vadose zone, topography, hydraulic conductivity, and land use
16 were used to calculate the DRASTIC and CDRASTIC indices. A sensitivity test was also
17 performed to determine the sensitivity of the parameters. Results showed that the topographic layer
18 displays a gentle slope in the aquifer. Most of the aquifer was covered with irrigated field crops
19 and grassland with a moderate vegetation cover. In addition, the aquifer vulnerability maps
20 indicated very similar results, identifying the northwest parts of the aquifer as areas with high to
21 very high vulnerability. The map removal sensibility analysis (MRSA) revealed the impact of the

22 vadose zone (in the DRASTIC index) and hydraulic conductivity (in the CDRASTIC index) as the
23 most important parameters in vulnerability evaluation. In both indices, the single-parameter
24 sensibility analysis (SPSA) demonstrated net recharge as the most effective factor in vulnerability
25 estimation. According to the results, parts of the studied aquifer have a high vulnerability and
26 require protective measures.

27 **Keywords:** Vulnerability; Sensitivity Analysis; DRASTIC; Composite DRASTIC; Kerman–
28 Baghin Aquifer

29 **1. Introduction**

30 Groundwater is a significant and principal freshwater resource in most parts of the world,
31 especially in arid and semi-arid areas. Water quality has been emphasized in groundwater
32 management (Neshat et al., 2014; Manap et al., 2013; Manap et al., 2014a; Ayazi et al., 2010). The
33 potential groundwater contamination by human activities at or near the surface of groundwater has
34 been considered the major basis for managing this resource by implementing preventative policies
35 (Tilahun and Merkel, 2010).

36 Groundwater vulnerability is a measure of how easy it is for pollution or contamination at the
37 land surface to reach a production aquifer. In other words, it is a measure of the “degree of
38 insulation” that natural and artificial factors provide to keep pollution away from the groundwater
39 (Sarah and Patricia, 1993; Neshat et al., 2014). Vulnerability maps are commonly plotted at the
40 sub-region and regional scales. Normally, they are not applied to site-specific evaluations,
41 including zones smaller than a few tens of square kilometers (Baalousha, 2006; Tilahun and
42 Merkel, 2010). Various techniques have been developed to assess groundwater susceptibility with
43 great precision (Javadi et al., 2010; Javadi et al., 2011). Most of these techniques are based on
44 analytic tools to associate groundwater contamination to land operations. There are three types of

45 evaluation methods: process-based simulations, statistic procedures, and overlay and index
46 approaches (Neshat et al., 2014; Dixon, 2004).

47 Process-based approaches involve numerical modeling and are useful at the local but not at
48 the regional level. Statistical approaches involve correlating actual water quality data to spatial
49 variables and require a large amount of site-specific data (National Research Council, 1993).
50 Overlay and index procedures emphasize the incorporation of various zonal maps by allocating a
51 numeral index. Both procedures are simple to implement in the GIS, especially on a zonal measure.
52 Hence, these methods are the most popular procedures applied for vulnerability estimation (Neshat
53 et al., 2014). The overlay and index methods have some significant advantages; first, they have
54 become popular because the methodology is fairly straightforward and can be easily implemented
55 with any GIS application software. The concept of overlaying data layers is easily comprehensible,
56 even by less experienced users. In addition, the data requirement can be considered as moderate,
57 since nowadays most data come in a digital format. Hydrogeological information is either available
58 or could be estimated using relevant data. Consequently, these methods yield relatively accurate
59 results for extensive areas with a complex geological structure. Last, the product of this approach
60 could be easily interpreted by water-resource managers and incorporated into decision-making
61 processes. Even a simple visual inspection of the vulnerability map can reveal important
62 contamination hotspots. Probably the most important and obvious disadvantage of these methods
63 raised by scientists and experts is the inherent subjectivity in the determination of the rating scales
64 and the weighting coefficients (National Research Council, 1993).

65 The most extensively used methods for groundwater vulnerability evaluation are GODS
66 (Ghazavi and Ebrahimi, 2015), IRISH (Daly and Drew, 1999), AVI (Raju et al., 2014), and
67 DRASTIC (Neshat et al., 2014; Baghapour et al., 2014; Baghapour et al., 2016).

68 The DRASTIC index, proposed by Aller et al. (1985), is regarded as one of the best indices
69 for groundwater vulnerability estimation. This method ignores the influence of zonal properties.
70 Thus, identical weights and rating values are utilized. In addition, this technique fails to apply a
71 standard validation test for the aquifer. Therefore, several investigators developed this index using
72 various techniques (Neshat et al., 2014). A higher DRASTIC index represents a greater
73 contamination potential, and vice versa. After calculating the DRASTIC index, it should be
74 possible to identify the zones that are more prone to pollution. This index only provides a relative
75 estimation and is not created to make a complete assessment (Baalousha, 2006).

76 Many studies have been conducted using the DRASTIC index to estimate groundwater
77 vulnerability in different regions of the world (Jaseela et al., 2016; Zghibi et al., 2016; Kardan
78 Moghaddam et al., 2017; Kumar et al., 2016; Neshat and Pradhan, 2017; Souleymane and Tang,
79 2017; Ghosh and Kanchan, 2016; Saida et al., 2017); however, there are still a number of studies
80 that have employed the CDRASTIC index for groundwater vulnerability evaluation (Baghapour
81 et al., 2016; Baghapour et al., 2014; Secunda et al., 1998; Jayasekera et al., 2011; Shirazi et al.,
82 2012; Jayasekera et al., 2008). Boughriba et al. (2010) utilized the DRASTIC index in a GIS
83 environment to estimate aquifer vulnerability. They provided the DRASTIC-modified map
84 prepared from total DRASTIC indices and small monitoring network maps including high and
85 medium classes. Then, they integrated the map with a land use map to prepare a contamination
86 potential map. They reported the newly obtained groundwater vulnerability map, including three
87 classes, namely very high, high, and medium. Babiker et al. (2005) used the DRASTIC index to
88 determine the points prone to contamination from human activities in the aquifer. They reported
89 that the western and eastern parts of the aquifer fall in the high and medium classes, respectively,
90 in terms of vulnerability. The final aquifer vulnerability map represented that a high risk of

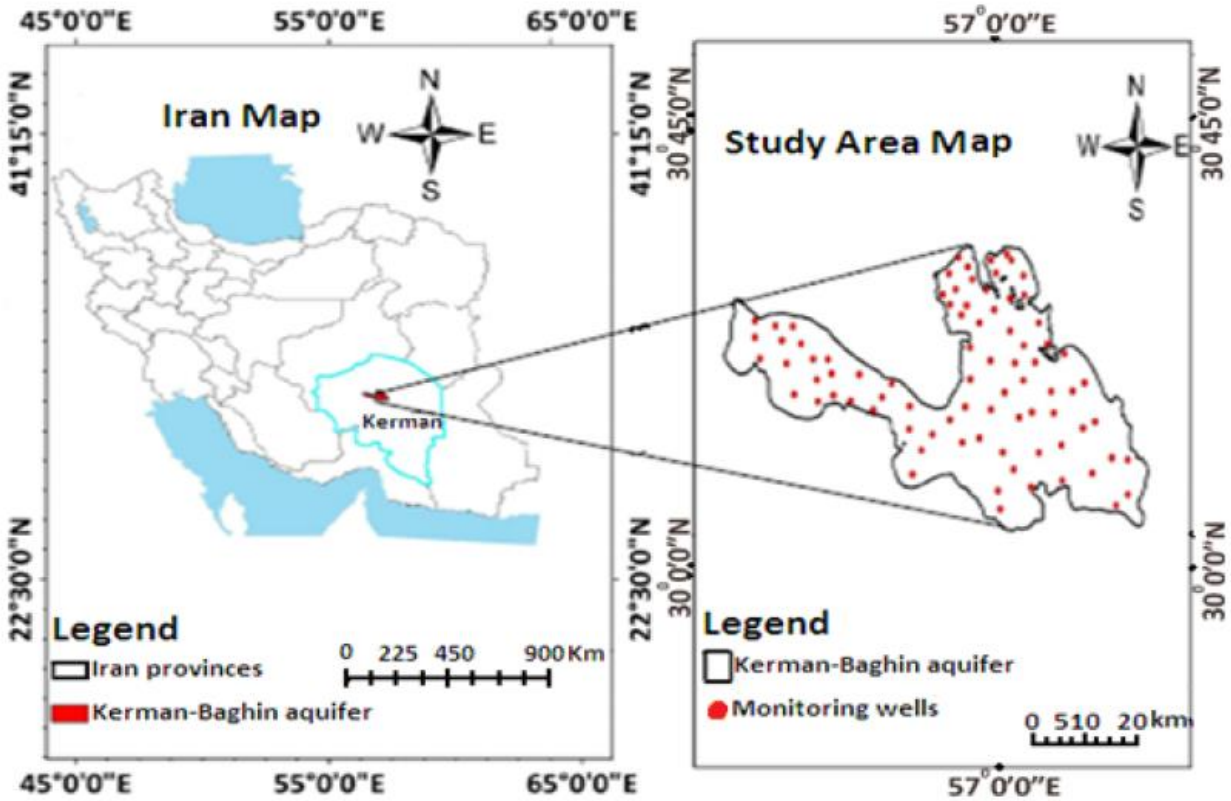
91 pollution is found in the eastern part of the aquifer due to agricultural activities. They also observed
92 that net recharge inflicts the largest impact on aquifer vulnerability, followed by soil media,
93 topography, the impact of the vadose zone, and hydraulic conductivity.

94 The average annual precipitation in Iran is 257 mm (less than one-third of the average annual
95 precipitation at the global level). Water scarcity is a critical problem in Iran (Chitsazan and
96 Akhtari, 2006; Modabberi et al., 2017), and groundwater reduction has exacerbated the problem.
97 Groundwater is the only freshwater resource in Kerman Province, Iran, due to the lack of surface
98 water. The Baghin aquifer is located in the central part of Kerman Province. Due to recent
99 droughts, this aquifer has been under heavy pumping stress to irrigate crops, which caused a
100 gradual drop in water level. Consequently, this could increase the contamination potential by
101 changing the physical and chemical properties of water in the aquifer. Therefore, the aim of this
102 research was to provide a vulnerability map for the Kerman–Baghin aquifer and perform a
103 sensitivity analysis to identify the most influential factors in vulnerability assessment.

104 **2. Materials and Methods**

105 **2.1. Study Area**

106 The Kerman province covers both arid and semi-arid lands. The present study included a 2023-
107 km² area (29° 47' to 30° 31' N latitude and 56° 18' to 57° 37' E longitude) located in the central
108 part of Kerman Province (Figure 1). The study area is mostly covered with agricultural lands
109 (Neshat et al., 2014). The mean annual rainfall is 108.3 mm (during 2017) in the study area; the
110 highest and lowest topographic elevation is 1,980 and 1,633 m above the sea level, respectively;
111 and the mean, minimum, and maximum annual temperatures equal 17°C, -12°C, and 41°C,
112 respectively (during 2017).



113

114 **Figure 1.** Location map of the Kerman–Baghin aquifer

115 **2.2. Computation of DRASTIC and CDRASTIC Indices**

116 DRASTIC is a procedure developed by the United States Environmental Protection Agency (U.S.
 117 EPA) to evaluate groundwater pollution (Aller et al., 1985). The DRASTIC index is obtained using
 118 the following equation (Kardan Moghaddam et al., 2017; Neshat and Pradhan, 2017):

119
$$\text{DRASTIC index} = D_r D_w + R_r R_w + A_r A_w + S_r S_w + T_r T_w + I_r I_w + C_r C_w \quad (1)$$

120 where DRASTIC comprises the effective factors in the DRASTIC index; D, R, A, S, T, I, and C
 121 stand for water table depth, net recharge, aquifer media, soil media, topography, the impact of the
 122 vadose zone, and hydraulic conductivity, respectively; and “r” and “w” denote the rating and
 123 weight of each factor, respectively. The ratings and weights of the factors are presented in Table
 124 1. A high DRASTIC index corresponds to the high vulnerability of the aquifer to pollution. In the
 125 DRASTIC index, each parameter is rated on a scale from 1 to 10 that shows the relative

126 contamination potential of that parameter for that area. In addition, in the DRASTIC index, one
 127 weight (1 to 5) is assigned to each parameter. Weight values indicate the relative significance of
 128 the parameters with respect to one another. Ranges of vulnerability corresponding to the
 129 DRASTIC index are presented in Table 2.

130 **Table 1** Ratings and weights related to DRASTIC index factors (Aller et al., 1985)

DRASTIC parameters	Range	Rating (r)	Weight (w)
Water table depth (m)	0.0–1.5	10	5
	1.5–4.6	9	
	4.6–9.1	7	
	9.1–15.2	5	
	15.2–22.9	3	
	22.9–30.5	2	
	>30.5	1	
Net recharge	11–13	10	4
	9–11	8	
	7–9	5	
	5–7	3	
	3–5	1	
Aquifer media	Rubble and sand	0	3
	Gravel and sand	7	
	Gravel, Sand, Clay and Silt	5	
	Sand and Clay	4	
	Sand, Clay and Silt	3	
Soil media	Rubble, Sand, Clay and Silt	9	2
	Gravel and Sand	7	
	Gravel, Sand, Clay and Silt	6	
	Sand	5	
	Sand, Clay and Silt	3	
Topography or slope (%)	0–2	10	1
	2–6	9	
	6–12	5	
	12–18	3	
	>18	1	
The impact of vadose zone	Rubble, Sand, Clay and Silt	9	5
	Gravel and Sand	7	
	Gravel, Sand, Clay and Silt	5	
	Sand, Clay and Silt	3	
Hydraulic conductivity (m/day)	0–4.1	1	3
	4.1–12.2	2	
	12.2–28.5	4	
	28.5–40.7	6	
	40.7–81.5	8	

131 **Table 2** Range of vulnerability related to the DRASTIC index

Vulnerability	Ranges
Very Low	23–46
Low	47–92
Moderate	93–136
High	137–184
Very high	>185

132 In the CDRASTIC index , the DRASTIC index is modified by adding a new parameter called land
 133 use. The role of land use in aquifer vulnerability potential is determined. Thus, the CDRASTIC
 134 index was obtained as follows:

135
$$\text{CDRASTIC index} = D_r D_w + R_r R_w + A_r A_w + S_r S_w + T_r T_w + I_r I_w + C_r C_w + L_r L_w \quad (2)$$

136 where L_w and L_r are the relative weight and rating related to land use, respectively. Ratings and
 137 weightings applied to the pollution potential are presented in Table 3 and are related to land use based
 138 on the CDRASTIC index. The final outputs of the CDRASTIC index range from 28 to 280.
 139 Vulnerability ranges based on the CDRASTIC index are presented in Table 4.

140 **Table 3** Ratings and weighting applied to the pollution potential related to land use based on the
 141 CDRASTIC index (Aller et al., 1985)

Land use	Rating	Weight
Irrigated field crops+ urban areas	10	
Irrigated field crops+ Grassland with poor vegetation cover+ urban areas	9	
Irrigated field crops+ Grassland with moderate vegetation cover+ urban areas	8	
Irrigated field crops	8	
Irrigated field crops+ Fallow land+ Grassland with moderate vegetation cover+ urban areas	7	
Irrigated field crops+ Grassland with poor vegetation cover	7	
Irrigated field crops+ Grassland with moderate vegetation cover	6	
Irrigated field crops+ Rocky+ urban areas	5	5
Irrigated field crops+ Grassland with poor vegetation cover+ Woodland	5	
Irrigated field crops+ Woodland	5	
Irrigated field crops+ Rocky	4	
Fallow land	3	
Fallow land+ Grassland with poor vegetation cover	3	
Fallow land+ Grassland with moderate vegetation cover	3	
Grassland with poor vegetation cover	2	
Grassland with moderate vegetation cover	2	
Grassland with moderate vegetation cover+ Woodland	1	
Sand dune+ Grassland with moderate vegetation cover	1	
Sand dune	1	

142

143 **Table 4** Vulnerability ranges related to the CDRASTIC index

Vulnerability	Ranges
Very Low	100
Low	100–145
Moderate	145–190
High	190–235
Very high	≥235

144 **2.3. Factors Affecting the Transfer of Contamination**

145 Water table depth is the distance of the water table from the ground surface in a well (Baghapour
 146 et al., 2016). Eighty-three wells were utilized in the Kerman–Baghin aquifer to obtain this factor.
 147 The interpolation procedure was adopted to provide a raster map of the water table depth, which
 148 was categorized based on Table 2.

149 Net recharge is the amount of runoff that has penetrated into the ground and has reached the
 150 groundwater surface (Singh et al., 2015; Ghosh and Kanchan, 2016). This research used the
 151 Piscopo method (Chitsazan and Akhtari, 2009) to provide a net recharge layer for the Kerman–
 152 Baghin aquifer according to the following equation and Table 5:

153
$$\text{Net recharge} = \text{slope (\%)} + \text{rainfall} + \text{soil permeability.} \quad (3)$$

154 In the above equation, the percentage of the slope was calculated from a topographical map,
 155 using a digital elevation model. In addition, a soil permeability map was created using the Kerman–
 156 Baghin aquifer soil map (scale of 1:250000) and the drilling logs of 83 wells. Finally, a map of the
 157 rainfall rate in the area was plotted based on annual average precipitation. The ratings and weights
 158 of net recharge are presented in Table 5.

159 **Table 5** Weight, rating, and range of net recharge (Aller et al., 1985)

Slope (%)		Rainfall		Soil permeability		Net Recharge		
Range (%)	Factor	Range (mm/year)	Factor	Range	Factor	Rang (cm/year)	Rating	Weight
<2	4	>850	4	High	5	11–13	10	
2–10	3	700–850	3	Moderate to High	4	9–11	8	
10–33	2	500–700	2	Moderate	3	7–9	5	4
>33	1	<500	1	Low	2	5–7	3	
				Very Low	1	3–5	1	

160 Aquifer media controls the movement of groundwater streams in the aquifer (Aller et al., 1985;
161 Singh et al., 2015). To obtain this layer, the drilling log data of 83 wells were used. Data were
162 collected from the Kerman Regional Water Office (KRWO). The range of the aquifer media layer
163 is shown in Table 2.

164 Soil media has a considerable impact on the amount of water surface that can penetrate the
165 aquifer. Therefore, where the soil layer is thick, the debilitation processes such as absorption,
166 filtration, degradation, and evaporation may be considerable (Singh et al., 2015). A soil media
167 raster map was provided using the Kerman–Baghin aquifer soil map and the wells’ drilling logs.
168 The range of the soil media layer is presented in Table 2.

169 Topography controls the residence time of water inside the soil and the degree of penetration
170 (Singh et al., 2015). To obtain this layer, the percentage of the slope was obtained from the
171 topographical map, using a digital elevation model. Data were collected from the KRWO. The
172 range of the topographic layer is presented in Table 2.

173 A vadose zone is an unsaturated area located between the topographic surface and the
174 groundwater level (Singh et al., 2015). It plays a significant role in decreasing groundwater
175 contamination by pollutant debilitation processes such as purification, chemical reaction, and
176 dispersal (Shirazi et al., 2012). This study used the lithologic data of 83 observation and
177 exploration wells to design the impact of the vadose zone raster map of the aquifer. The data were
178 collected from the KRWO. The range of the impact of the vadose zone layer is depicted in Table
179 2.

180 Hydraulic conductivity refers to the capability of the aquifer to transfer water. Areas with a high
181 hydraulic conductivity demonstrate a high potential for groundwater contamination (Singh et al.,

182 2015; Aller et al., 1985). To prepare this layer, data derived from pumping tests of wells were
183 used. The range of the hydraulic conductivity layer is given in Table 2.

184 Land use affects groundwater resources through changes in recharge and by changing demands
185 for water. Land use is obligatory since it is required by the CDRASTIC index. The Indian remote
186 sensing satellite information was utilized to create the land use raster map. The weight and rating
187 related to the land use layer are presented in Table 3.

188 **2.4. Sensitivity Analyses**

189 One of the main advantages of the DRASTIC index is the evaluation performance because a high
190 number of input data are used, and this helps restrict the effects of errors on final results.
191 Nevertheless, some authors, namely Babiker et al. (2005), Barber et al.(1993), and Merchant
192 (1994), reported that similar results could be obtained using fewer data and at lower costs. The
193 unavoidable subjectivity related to the selection of seven factors, ranks, and weights used to
194 calculate the vulnerability index has also been criticized. Therefore, in order to eliminate the
195 aforementioned criticisms, two sensitivity analyses were performed as follows (Napolitano and
196 Fabbri, 1996):

197 **A. Map Removal Sensibility Analysis (MRSA)**

198 MRSA value indicates the vulnerability map's sensibility to the removal of one or more maps from
199 the suitability analysis. MRSA is calculated as follows (Babiker et al., 2005; Martínez-Bastida et
200 al., 2010; Saidi et al., 2011; Modabberi et al., 2017):

$$201 \quad S = \left[\left| \frac{\frac{V}{N} - \frac{V'}{n}}{V} \right| \right] \times 100 \quad (4)$$

202 where S stands for the sensibility value expressed in terms of the variation index, V is the intrinsic
203 vulnerability index (real vulnerability index), V' is the intrinsic vulnerability index after removing

204 X, and N and n are the number of data pieces used to calculate V and V', respectively (Babiker et
205 al., 2005; Martínez-Bastida et al., 2010; Saidi et al., 2011; Modabberi et al., 2017).

206 **B. Single-Parameter Sensibility Analysis (SPSA)**

207 SPSA was first introduced by Napolitano and Fabbri (1996). This test shows the effect of each
208 DRASTIC factor on the final vulnerability index. Using this test derived from Equation 5, the real
209 and effective weight of each factor, compared to the theoretical weight assigned by the analytical
210 model, was calculated by Babiker et al. (2005), Martínez-Bastida et al.(2010), Saidi et al. (2011),
211 and Modabberi et al.(2017);

$$212 W = \left[\frac{P_r P_w}{V} \right] \times 100 \quad (5)$$

213 where W represents the effective weight of each factor, P_r and P_w are the rank and weight assigned
214 to P, respectively, and V denotes the intrinsic vulnerability index (Martínez-Bastida et al., 2010;
215 Babiker et al., 2005; Saidi et al., 2011; Modabberi et al., 2017).

216 **3. Results and Discussion**

217 **3.1. DRASTIC and CDRASTIC Parameters**

218 Based on the data shown in Table 2, the assigned rating of water table depth varies from 1 to 10.
219 In addition, based on the results presented in Table 6, water table depth in the aquifer varies from
220 4.6 to >30.5 m (rating 1 to 7). About 27.55% of the aquifer has a depth >30.5 m, and 66.16% of
221 the aquifer has a depth ranging from 9.1 m to 30.5 m. Less than 7% of the aquifer has a depth
222 between 4.6 m and 9.1 m. The Kerman–Baghin aquifer rated map of water table depth is depicted
223 in Figure 2(A). According to Figure 2(A) and Table 6, the minimum impact of water table depth
224 on aquifer vulnerability occurs in the central parts (6.39%), whereas the maximum impact occurs
225 in the northern, southern, northwestern, and southeastern parts (27.55%).

226 According to the results presented in Table 6, 75.81% of the aquifer has a net recharge value of
227 7 to 9 cm/year. A net recharge value between 9 and 11 cm/year was found for 11.74% of the
228 aquifer. The Kerman–Baghin aquifer rated map of net recharge is illustrated in Figure 2(B).
229 According to Piscopo's method, the Kerman–Baghin aquifer was divided into three classes with
230 regard to net recharge. The highest net recharge value was observed in the northern, northeastern,
231 southern, and southwestern parts of the northwest, parts of the center, and parts of the southeast
232 (75.81%), whereas the least net recharge value appeared in parts of the northwest and center
233 (11.74%), as shown in Figure 2(B) and Table 6.

234 As observed in Table 6, the majority of the Kerman–Baghin aquifer media is composed of sand,
235 clay, and silt (75.21%). The Kerman–Baghin aquifer rated map of the aquifer media is presented
236 in Figure 3(A). Parts of the aquifer in the north, northwest, northeast, center, and southeast are
237 composed of sand, clay, and silt. Parts of the aquifer in the northwest are composed of rubble and
238 sand (5.58%). Parts of the aquifer in the south and northwest are composed of gravel and sand
239 (8.95%), and gravel, sand, clay, and silt (10.26%).

240 The Kerman–Baghin aquifer rated map of soil media is presented in Figure 3(B). The soil map
241 depicts six soil classes. The highest rank (rank = 9) was assigned to rubble, sand, clay, and silt (a
242 combination of rubble, sand, clay and silt soils). In addition, the lowest rank (rank = 2) was
243 assigned to clay and silt (a combination of clay and silt soils). Most of the aquifer soil media is
244 covered with silt, sand, and clay (about 80%).

245 The Kerman–Baghin aquifer rated map of topography is shown in Figure 4(A). The
246 topographical layer demonstrates a gentle slope (0 to 6%) over most of the aquifer, hence gaining
247 the ranks of 9 and 10. A slope range of 0 to 2% includes 34.72% of the study area, and its rating
248 (slope range = 0–2%) is 10. In addition, 65.28% of the aquifer has a slope range of 2 to 6% (parts

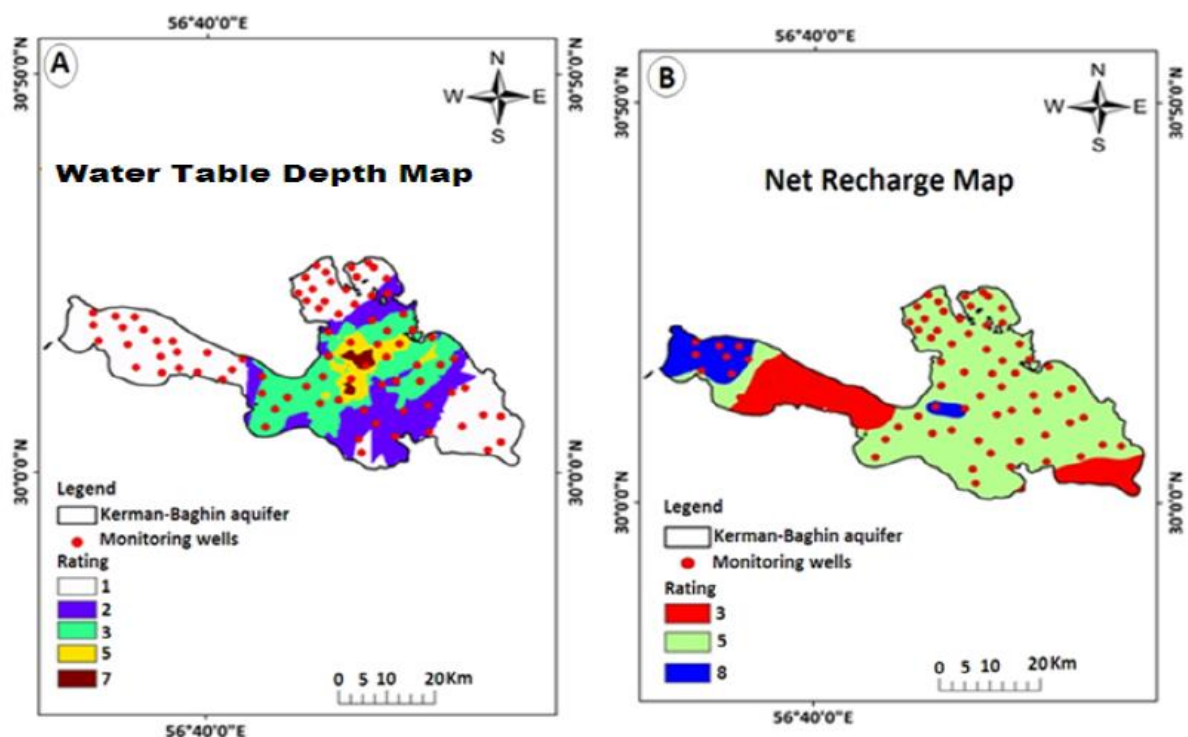
249 of the northwest) as shown in Figure 4(A) and Table 6. As the gradient increases, the runoff
250 increases as well (Israil et al., 2006), leading to less penetration (Jaiswal et al., 2003). According
251 to Madrucci et al. (2008), the gradients higher than 35° are considered restrictions on groundwater
252 desirability because of the lack of springs.

253 The Kerman–Baghin aquifer rated map of the impact of the vadose zone is indicated in Figure
254 4(B). According to the results, the soil with a rank of 5 (gravel, sand, clay, and silt) is more
255 effective on aquifer vulnerability (35.47%). Other types of soils such as sand, clay, and silt (parts
256 of the north, northeast, south, and southeast), gravel and sand (parts of the center and northwest),
257 and rubble, sand, clay, and silt (parts of the northwest) cover 34.24%, 20.39%, and 9.9% of the
258 aquifer, respectively, as shown in Figure 4(B) and Table 6. Sandy soil is effective on groundwater
259 occurrence because of the high rate of penetration (Srivastava and Bhattacharya, 2006). However,
260 clay soil is arranged poorly because of low infiltration (Manap et al., 2014b).

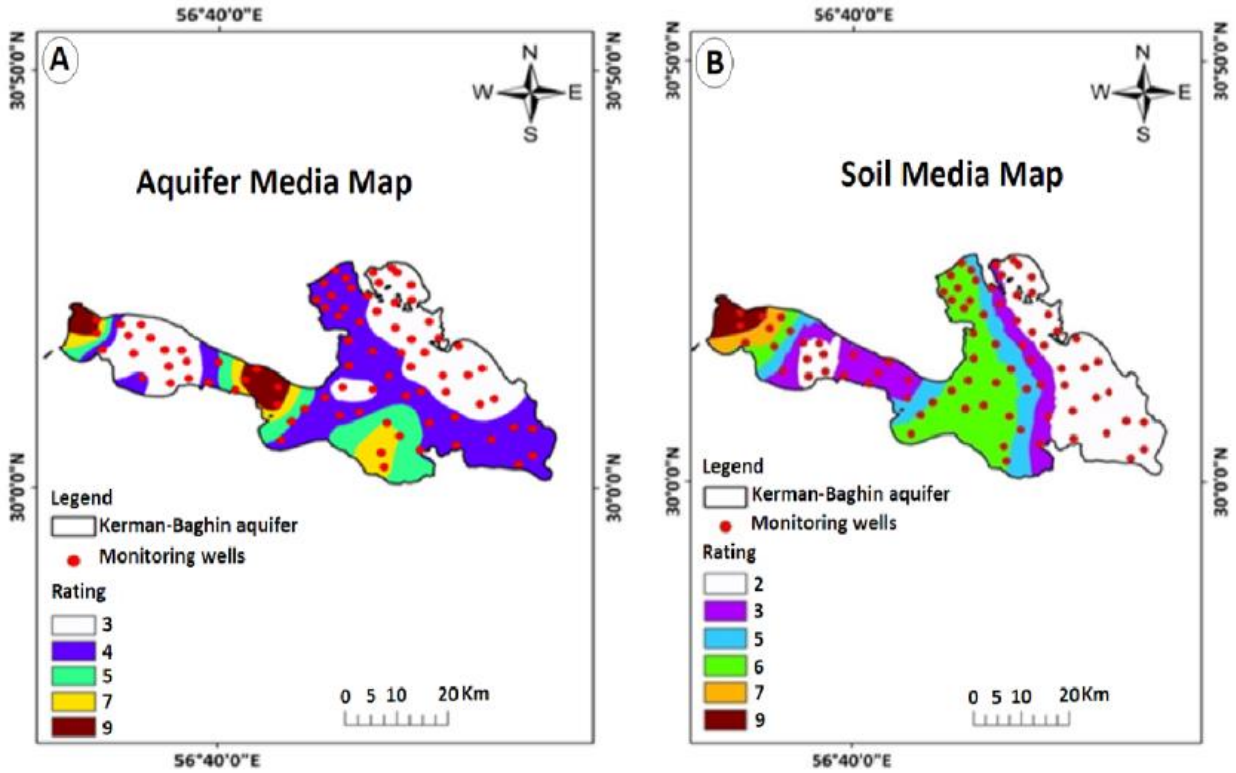
261 The Kerman–Baghin aquifer rated map of hydraulic conductivity is illustrated in Figure 5(A).
262 Hydraulic conductivity shows a high degree of variability. The findings showed that the hydraulic
263 conductivity of the Kerman–Baghin aquifer varies from 0 to 81.5 m/day. The potential for
264 groundwater contamination was greater in zones with high hydraulic conductivity (38.27%). As
265 shown in Figure 5(A) and Table 6, 29.51%, 23.93%, 5.98%, and 2.31% of the study areas have
266 hydraulic conductivity in the ranges of 0 to 4.1 m/day, 12.2 to 28.5 m/day, 28.5 to 40.7 m/day, and
267 40.7 to 81.5 m/day, respectively.

268 The Kerman–Baghin aquifer rated map of land use is presented in Figure 5(B). The results
269 indicated that the majority of the Kerman–Baghin aquifer is covered with irrigated field crops and
270 grassland with a moderate vegetation cover (20.45%). Less than 4% of the study area is composed
271 of irrigated field crops and urban areas (3.61%), and 58.47% of the study area consists of irrigated

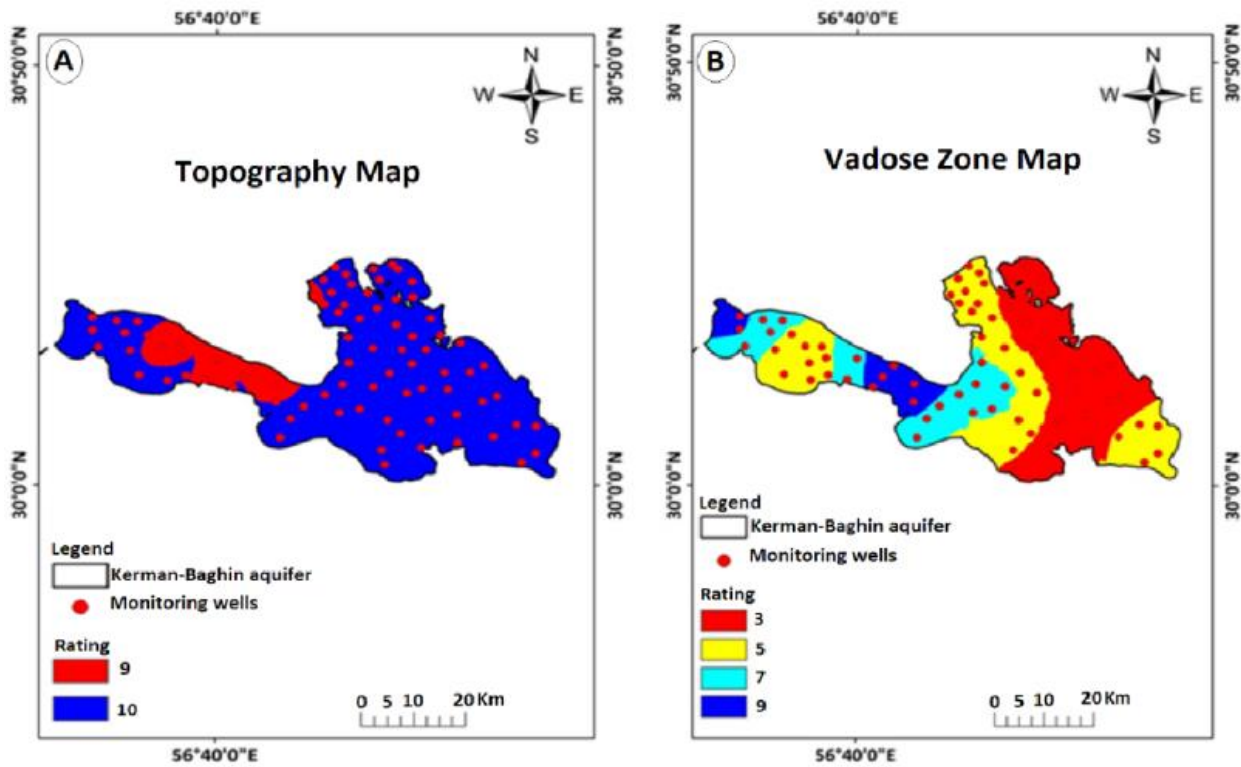
272 field crops with urban areas, grassland with poor and moderate vegetation cover, fallow land,
273 woodland, and rocky ground. In addition, 10.17% of the study area is fallow land with poor
274 grassland and moderate vegetation, and 13.72% of the study area is sand dunes with poor grassland
275 and moderate vegetation cover and woodland, as displayed in Figure 5(B) and Tables 3 and 6.



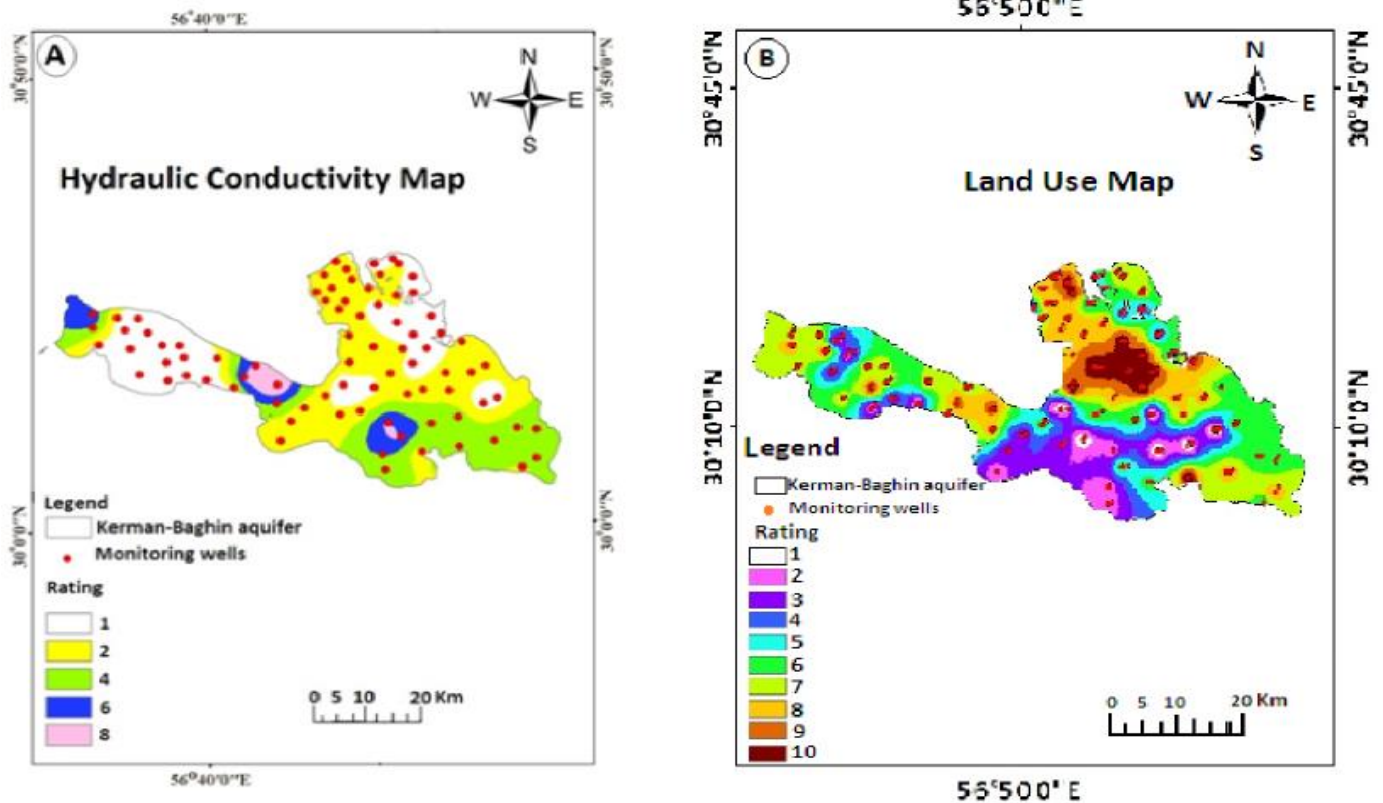
276
277 **Figure 2.** The Kerman–Baghin aquifer rated maps of A) water table depth and B) net recharge



278
 279 **Figure 3.** The Kerman–Baghin aquifer rated maps of A) aquifer media and B) soil media
 280



281
 282 **Figure 4.** The Kerman–Baghin aquifer rated maps of A) topography and B) vadose zone



283
284 **Figure 5.** The Kerman–Baghin aquifer rated maps of A) hydraulic conductivity and B) land use

285 **Table 6** Area of rating (km² and %) of DRASTIC and CDRASTIC parameters

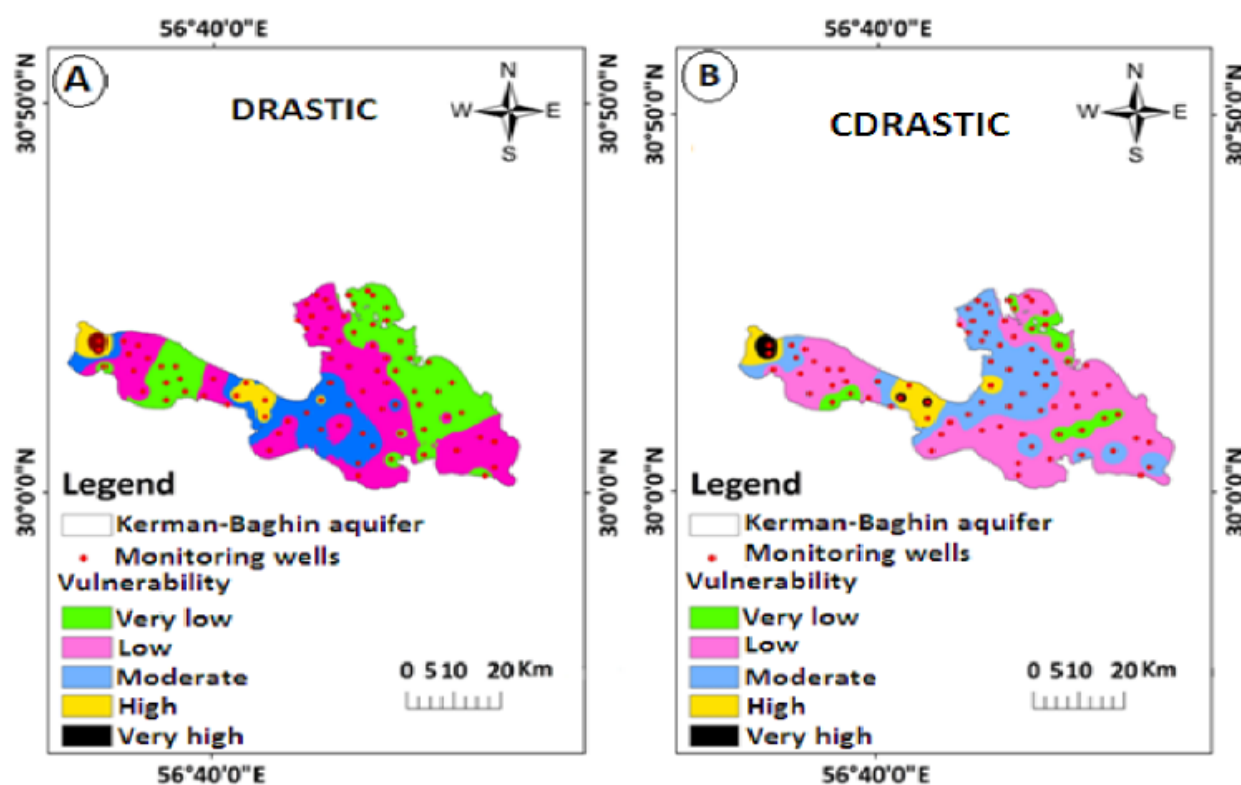
DRASTIC and DRASTIC indexes parameters	Rating	Area (km²)	Area (%)	The aquifer geographic directions covered by the respective rating in the parameters rated maps
Water table depth	1	557.73	27.55	Parts of the north, south, northwest, and southeast
	2	472.18	23.34	Parts of the north, south and center
	3	469.78	23.29	Parts of the center
	5	395.00	19.53	Parts of the center
	7	129.14	6.39	Parts of the center
Net recharge	3	252.04	12.45	Parts of southeast, and northwest
	5	1534.15	75.81	North, northeast, south, southwest, and part of the northwest, center, southeast
Aquifer media	8	237.6	11.74	Parts of the northwest and center
	3	743.18	36.72	Parts of the north, northwest, northeast, and center
	4	779.01	38.49	Parts of the north, northwest, southeast, and center
	5	207.81	10.26	Parts of the south, and northwest
	7	181.02	8.95	Parts of the south, and northwest
Soil media	9	112.76	5.58	Parts of the northwest
	2	658.5	32.53	Parts of the north, northwest, northeast, and southeast
	3	399.72	19.75	Parts of the north, northwest, south, and center
	5	297.44	14.69	Parts of the north, northwest, south, and center
	6	538.77	26.62	Parts of the northwest, center, and southwest
	7	67.56	3.33	Parts of the northwest
	9	61.79	3.08	Parts of the northwest

Topography	9	702.74	34.72	North, northwest, northeast, South, southeast, southwest, and center
	10	1321.07	65.28	Parts of the northwest
The impact of the vadose zone	3	692.87	34.24	Parts of the north, northeast, south, and southeast
	5	717.91	35.47	Parts of the north, northwest, south, southeast, and center
Hydraulic conductivity	7	412.49	20.39	Parts of the center and northwest
	9	200.53	9.9	Parts of the northwest
	1	597.11	29.51	Parts of the northeast, northwest, southeast, and center
	2	774.52	38.27	Parts of the northwest, south, southeast and center
	4	484.17	23.93	Parts of the northwest, south and southeast
	6	120.99	5.98	Parts of the south, northwest
Land use	8	46.7	2.31	Parts of the south, northwest
	1	112.48	5.56	Parts of the south
	2	165.02	8.16	Parts of the south
	3	205.65	10.17	Parts of the south and center
	4	357.06	17.64	Parts of the south, southwest, northwest, and center
	5	234.86	11.61	Parts of the southeast, northwest, and center
	6	413.86	20.45	Parts of the southeast, northwest, northeast and center
	7	182.63	9.02	Parts of the north, northwest, northeast
	8	169.04	8.37	Parts of the north, northwest, northeast
	9	109.42	5.41	Parts of the north, northwest, northeast
	10	73.09	3.61	Parts of the north

286 **3.2. DRASTIC and CDRASTIC Vulnerability Indices**

287 The Kerman–Baghin aquifer vulnerability map obtained using DRASTIC and CDRASTIC indices
288 is given in Figure 6. In the studied aquifer, vulnerability falls under very high, high, moderate,
289 low, and very low vulnerable areas. It is found that in both indices, the northern, northeastern,
290 northwestern, southern, southwestern, southeastern, and central parts are classified as having low
291 and very low vulnerability. This could be attributed to the low water depth, hydraulic conductivity,
292 and net recharge characterizing these aquifer areas; another reason might be that the aquifer media
293 is mostly clay, sand, and silt soils. The vulnerability area, identified by the investigated indices, is
294 illustrated in Table 7. Zones with a low and very low vulnerability cover 25.21% and 38.31% of
295 the Kerman–Baghin aquifer, respectively, using DRASTIC index. Very low and low-vulnerability
296 zones cover 24.95% and 40.41%, respectively, using the CDRASTIC index. This is primarily due
297 to water table depth and the relatively low permeability of the vadose zone in those aquifers (Colins
298 et al., 2016). A bout 26% of the studied aquifer had moderate groundwater pollution potential,

299 using DRASTIC and CDRASTIC indices. This does not mean that these areas are without
 300 pollution; rather, they are relatively prone to pollution when compared to other areas (Colins et al.,
 301 2016). From the DRASTIC index values, it was found that 10.4% of the studied aquifer had high
 302 (8.46%) and very high (1.94%) vulnerability. The results revealed that 8.75% of the aquifer fell in
 303 the range of 190 to 235 and greater than 235 in the CDRASTIC index (Table 7). According to
 304 these two indices, the vulnerability maps indicated very similar findings, suggesting that the
 305 northwestern part of the aquifer has zones with high and very high vulnerability. The high
 306 vulnerability can be attributed to great water depth, hydraulic conductivity, and net recharge in
 307 these aquifer areas. In addition, this can due to the great slope in this area.



308
 309 **Figure 6.** Vulnerability maps of the Kerman–Baghin aquifer by DRASTIC and CDRASTIC
 310 indices

311 **Table 7** Area of vulnerability (km² and %) identified by DRASTIC and CDRASTIC indices

DRASTIC

CDRASTIC

Vulnerability	Rating	Area (km ²)	Area (%)	The aquifer geographic directions covered by the respective Vulnerability	Rating	Area (km ²)	Area (%)	The aquifer geographic directions covered by the respective Vulnerability
Very Low	23–46	510.25	25.21	Parts of the south, north, northwest, and northeast	<100	505.02	24.95	Parts of the southeast, north, northwest, and northeast
Low	47–92	775.14	38.31	Parts of the south, southwest, southeast, north, northwest, northeast, and center	100–145	817.70	40.41	Parts of the south, southwest, southeast, north, northwest, northeast, and center
Moderate	93–136	527.85	26.08	Parts of the south, southwest, northwest, and center	145–190	524.06	25.89	Parts of the south, southwest, southwest, northwest, and center
High	137–184	171.02	26.08	Parts of the northwest	190–235	126.91	6.28	Parts of the northwest and center
Very high	>185	39.23	1.94	Parts of the northwest	≥235	49.79	2.47	Parts of the northwest

312 3.3. Sensitivity of the DRASTIC Index

313 The MRSA, the DRASTIC index, is performed by eliminating the data of one layer at a time as
314 indicated in Table 8. The results showed a high variation in the vulnerability index when the impact
315 of the vadose zone was removed, such that the average variation index was 1.88%. This shows
316 that the factor is more effective in vulnerability assessment using the DRASTIC index. When this
317 parameter is removed from the overlay process, a significant decrease was observed in the
318 vulnerability index. This could be due to the high theoretical weight assigned to this factor (weight
319 = 5). These findings are similar to those obtained by Dibi et al. (2012) who have shown that, in
320 addition to this parameter, topography, net recharge, and water table depth have a high impact on
321 the vulnerability index. In addition, according to Samake et al. (2011), the vadose zone and
322 hydraulic conductivity had a significant impact on the vulnerability index, that appears to have a
323 moderate sensitivity to the deletion of water table depth (1.48%), net recharge (1.36%), and
324 hydraulic conductivity (1.25%). The minimum menu variation index was achieved after
325 eliminating the aquifer media (0.44%), as indicated in Table 8.

326 To estimate the effect of individual factors on aquifer vulnerability, the SPSA was performed.
327 A summary of the results of SPSA in the DRASTIC index is given in Table 9. The SPSA compares

328 the effective and theoretical weights. The average effective weight of the net recharge was 43.26%,
 329 and its theoretical weight (%) was 17.4%. This shows that the factor is more effective in
 330 vulnerability assessment using the DRASTIC index. The results reported by other studies (Babiker
 331 et al., 2005; Doumouya et al., 2012) are similar to those of the present study. The water table depth
 332 and impact of the vadose zone parameters had high theoretical weights (21.74%), and have
 333 received an effective weight with the average value of 8.33% and 25.55% (Table 9). The remaining
 334 factors demonstrated an average effective weight of 14.91% (aquifer media), 9.89% (soil media),
 335 11.35% (topography), and 7.01% (hydraulic conductivity). The theoretical weights assigned to the
 336 water table depth, net recharge, topography, and hydraulic conductivity were not in agreement
 337 with the effective weight. The highest and lowest impact on aquifer vulnerability belonged to net
 338 recharge and hydraulic conductivity, respectively (Table 9).

339 **Table 8** Statistical results of MRSA in the DRASTIC index

SD	The sensitivity of variability index (S) (%)			Removed parameters
	Min.	Max.	Ave.	
0.414	0.05	2.36	1.36	D
0.775	0.07	3.06	1.48	R
0.311	0.05	1.31	0.44	A
0.486	0.00	1.65	0.73	S
0.339	0.03	1.31	0.51	T
0.894	0.25	3.84	1.88	I
0.550	0.03	1.98	1.25	C

340 **Table 9** Statistical results of SPSA in the DRASTIC index

SD	Effective weight (%)			Theoretical weight (%)	Theoretical Weight	Parameters
	Min.	Max.	Ave.			
6.179	3.23	28.46	8.33	21.74	5	D
11.998	14.06	73.47	43.26	17.4	4	R
3.190	7.26	22.13	14.91	13.04	3	A
2.916	4.49	14.29	9.89	8.7	2	S
2.222	6.45	14.71	11.35	4.3	1	T
5.367	15.79	37.31	25.55	21.74	5	I
3.738	2.42	18.75	7.01	13.04	3	C

341 **3.4. Sensitivities of the CDRASTIC index**

342 The MRSA in the CDRASTIC index was performed by eliminating one data layer at a time, as
 343 indicated in Table 10. The mean variation index of hydraulic conductivity was 4.13%. Hydraulic
 344 conductivity had the greatest effect on the aquifer vulnerability, followed by water table depth
 345 (4.05%), soil media (3.82%), topography (3.68%), aquifer media (3.28%), net recharge (2.72%),
 346 the impact of the vadose zone (2.33%), and land use (1.99%).

347 The effective weight derived from the SPSA to the CDRASTIC index is shown in Table 11.
 348 The average effective weight of net recharge was 32.62%. This shows that the factor is more
 349 effective in vulnerability assessment using CDRASTIC index. Hydraulic conductivity displays the
 350 lowest effective weight (5.32%). Topography, net recharge, and land use parameters had the
 351 maximum effective weights with respect to the theoretical weights specified for them. The average
 352 effective weight of land use was 24.82%. This suggests that the parameter was the second effective
 353 parameter in aquifer vulnerability, using the CDRASTIC index (Table 11).

354 **Table 10** Statistical results of MRSA in the CDRASTIC index

The sensitivity of variability index (S) (%)				Removed parameters
SD	Min.	Max.	Ave.	
1.403	0.50	6.48	4.05	D
1.617	0.11	10.91	2.72	R
1.541	0.06	5.99	3.28	A
1.508	0.67	6.60	3.82	S
1.353	0.87	5.87	3.68	T
1.439	0.06	5.12	2.33	I
1.480	0.55	6.72	4.13	C
0.375	1.23	3.00	1.99	L

355 **Table 11** Statistical results of SPSA in the CDRASTIC index

Effective weight (%)				Theoretical weight (%)	Theoretical Weight	Parameters
SD	Min.	Max.	Ave.			
4.849	2.63	26.88	6.27	21.74	5	D
10.672	10.4	66.67	32.62	17.4	4	R
3.026	6.29	20.00	11.23	13.04	3	A
2.621	3.31	12.96	7.5	8.7	2	S
1.609	5.2	12.82	8.45	4.3	1	T
4.648	10.87	32.05	19.2	21.74	5	I
3.134	2.1	14.88	5.32	13.04	3	C
10.122	3.88	42.37	24.82	17.85	5	L

356 **4. Conclusion**

357 Evaluations of vulnerability indices for the Kerman–Baghin aquifer were conducted using the GIS-
358 based DRASTIC and CDRASTIC indices. Seven hydro–geological factors (as the letters of the
359 acronym show) were considered in the determination of aquifer vulnerability using DRASTIC,
360 and eight parameters were considered in the CDRASTIC approach. From the DRASTIC index
361 values, it was determined that 10.4% of the aquifer has high (8.46%) to very high (1.94%)
362 vulnerability. From the CDRASTIC index values, it was determined that 8.75% of the aquifer has
363 high (6.28%) to very high (2.47%) vulnerability. In addition, we found that parts of the north,
364 south, southeast, and northwest have low to very low vulnerability based on the DRASTIC and
365 CDRASTIC indices. The MRSA signifies that hydraulic conductivity and the impact of the vadose
366 zone induce a high risk of aquifer contamination according to the DRASTIC and CDRASTIC
367 indices, respectively. For both methods, the SPSA analysis revealed that net recharge has a high
368 risk of aquifer contamination. Based on the results, parts of the Kerman–Baghin aquifer tend to be
369 contaminated, a point which merits the attention of regional authorities. Regarding urban planning
370 and the organization of agricultural activities in Kerman Province, the vulnerability map prepared
371 in this study could be valuable in the protection of groundwater quality. In areas with high and
372 very high vulnerability to groundwater pollution, there should be restrictions on soil fertilization
373 as well as permanent pasture, or afforestation should be introduced in the arable land. In addition,
374 these areas should not be converted into housing developments. Groundwater vulnerability maps
375 of the Kerman–Baghin aquifer are ideal for use in future land-use planning.

376 *Data availability.* Data can be shared at this stage as authors are currently analysing for further
377 work.

378 *Author contributions.* MN constructed an idea, planned methodology, interpreted results, and then
379 reached conclusions. MM supervised the whole process and provided personal, environmental,
380 and financial support for the research work. MN took responsibility for literature review and
381 finalising the whole paper and in the end critically reviewed the paper before submission.

382 *Acknowledgments.* The authors would like to thank the Environmental Health Engineering
383 Research Center, Kerman University of Medical Sciences, for their scientific support.

384 *Competing interests.* The authors declare that they have no conflict of interest.

385 **References**

386 Aller, L., Truman, b., Jay H, L., Rebeeca J, P., and Glen, H.: DRASTIC: a standardized system
387 for evaluating ground water pollution potential using hydrogeologic settings, U.S Environmental
388 Protection Agency, USA, 1985.

389 Ayazi, M. H., Pirasteh, S., Arvin, A., Pradhan, B., Nikouravan, B., and Mansor, S.: Disasters and
390 risk reduction in groundwater: Zagros Mountain Southwest Iran using geoinformatics techniques,
391 Disaster Adv., 3, 51-57, 2010.

392 Baalousha, H.: Vulnerability assessment for the Gaza Strip, Palestine using DRASTIC, J. Environ.
393 Geol., 50, 405-414, <https://doi.org/10.1007/s00254-006-0219-z>, 2006.

394 Babiker, I. S., Mohamed, M. A., Hiyama, T., and Kato, K.: A GIS-based DRASTIC model for
395 assessing aquifer vulnerability in Kakamigahara Heights, Gifu Prefecture, central Japan, Sci Total
396 Environ., 345, 127-140, <https://doi.org/10.1016/j.scitotenv.2004.11.005>, 2005.

397 Baghapour, M. A., Talebbeydokhti, N., Tabatabee, H., and Nobandegani, A. F.: Assessment of
398 groundwater nitrate pollution and determination of groundwater protection zones using DRASTIC
399 and composite DRASTIC (CD) models: the case of Shiraz unconfined aquifer, J. Health. Sci.
400 Surveill. Syst., 2, 54-65, 2014.

401 Baghapour, M. A., Nobandegani, A. F., Talebbeydokhti, N., Bagherzadeh, S., Nadiri, A. A.,
402 Gharekhani, M., and Chitsazan, N.: Optimization of DRASTIC method by artificial neural
403 network, nitrate vulnerability index, and composite DRASTIC models to assess groundwater
404 vulnerability for unconfined aquifer of Shiraz Plain, Iran, *J Environ Health Sci Eng.*, 14, 1-16,
405 <https://doi.org/10.1186/s40201-016-0254-y>, 2016.

406 Barber, C., Bates, L. E., Barron, R., and Allison, H.: Assessment of the relative vulnerability of
407 groundwater to pollution: a review and background paper for the conference workshop on
408 vulnerability assessment, *AGSO J Aust Geol Geophys.*, 14, 147-154, 1993.

409 Boughriba, M., Barkaoui, A.-e., Zarhloule, Y., Lahmer, Z., El Houadi, B., and Verdoya, M.:
410 Groundwater vulnerability and risk mapping of the Angad transboundary aquifer using DRASTIC
411 index method in GIS environment, *Arab J Geosci.*, 3, 207-220, [https://doi.org/10.1007/s12517-](https://doi.org/10.1007/s12517-009-0072-y)
412 [009-0072-y](https://doi.org/10.1007/s12517-009-0072-y), 2010.

413 Chitsazan, M., and Akhtari, Y.: Evaluating the potential of groundwater pollution in Kherran and
414 Zoweircherry plains through GIS-based DRASTIC model, *J. Water. Wastewater*, 17, 39-51, 2006.

415 Chitsazan, M., and Akhtari, Y.: A GIS-based DRASTIC model for assessing aquifer vulnerability
416 in Kherran Plain, Khuzestan, Iran, *Water Resour Manag.*, 23, 1137-1155,
417 <https://doi.org/10.1007/s11269-008-9319-8>, 2009.

418 Colins, J., Sashikkumar, M., Anas, P., and Kirubakaran, M.: GIS-based assessment of aquifer
419 vulnerability using DRASTIC Model: A case study on Kodaganar basin, *Earth Sci. Res. J.*, 20, 1-
420 8, <https://doi.org/10.15446/esrj.v20n1.52469>, 2016.

421 Daly, D., and Drew, D.: Irish methodologies for karst aquifer protection, in: Beek B (ed)
422 *Hydrogeology and engineering geology of sinkholes and karst*, Balkema, Rotterdam, 267-272,
423 1999.

424 Dibi, B., Kouame, K. I., Konan-Waidhet, A. B., Savane, I., Biemi, J., Nedeff, V., and Lazar, G.:
425 Impact of agriculture on the quality of groundwater resources in peri-urban zone of Songon (Cote
426 D'ivoire), *Environ. Engine. Manage. J.*, 11, 2173-2182, <https://doi.org/10.30638/eej.2012.271>,
427 2012.

428 Dixon, B.: Prediction of ground water vulnerability using an integrated GIS-based Neuro-Fuzzy
429 techniques, *J. Spat. Hydro.*, 4, 1-38, 2004.

430 Doumouya, I., Dibi, B., Kouame, K. I., Saley, B., Jourda, J. P., Savane, I., and Biemi, J.: Modelling
431 of favourable zones for the establishment of water points by geographical information system
432 (GIS) and multicriteria analysis (MCA) in the Aboisso area (South-east of Côte d'Ivoire), *Environ.*
433 *Earth. Sci.*, 67, 1763-1780, <https://doi.org/10.1007/s12665-012-1622-2>, 2012.

434 Ghazavi, R., and Ebrahimi, Z.: Assessing groundwater vulnerability to contamination in an arid
435 environment using DRASTIC and GOD models, *Inte. J. Environ. Sci. Tech*, 12, 2909-2918,
436 <https://doi.org/10.1007/s13762-015-0813-2>, 2015.

437 Ghosh, T., and Kanchan, R.: Aquifer vulnerability assessment in the Bengal alluvial tract, India,
438 using GIS based DRASTIC model, *Model Earth Syst Environ.*, 2, 2-13,
439 <https://doi.org/10.1007/s40808-016-0208-5>, 2016.

440 Israil, M., Al-hadithi, M., Singhal, D., Kumar, B., Rao, M. S., and Verma, S.: Groundwater
441 resources evaluation in the Piedmont zone of Himalaya, India, using Isotope and GIS techniques,
442 *J. Spatial. Hydro.*, 6, 107-119, 2006.

443 Jaiswal, R., Mukherjee, S., Krishnamurthy, J., and Saxena, R.: Role of remote sensing and GIS
444 techniques for generation of groundwater prospect zones towards rural development—an
445 approach, *Int J Remote Sens.*, 24, 993-1008, <https://doi.org/10.1080/01431160210144543>, 2003.

446 Jaseela, C., Prabhakar, K., and Harikumar, P. S. P.: Application of GIS and DRASTIC modeling
447 for evaluation of groundwater vulnerability near a solid waste disposal site, *Int. J. Geosci.*, 7,
448 558-571, <https://doi.org/10.4236/ijg.2016.74043>, 2016.

449 Javadi, S., Kavehkar, N., Mousavizadeh, M., and Mohammadi, K.: Modification of DRASTIC
450 model to map groundwater vulnerability to pollution using nitrate measurements in agricultural
451 areas, *J. Agr. Sci. Tech.*, 13, 239-249, 2010.

452 Javadi, S., Kavehkar, N., Mohammadi, K., Khodadadi, A., and Kahawita, R.: Calibrating
453 DRASTIC using field measurements, sensitivity analysis and statistical methods to assess
454 groundwater vulnerability, *Water. Int.*, 36, 719-732,
455 <https://doi.org/10.1080/02508060.2011.610921>, 2011.

456 Jayasekera, D., Kaluarachchi, J. J., and Villholth, K. G.: Groundwater Quality Impacts Due to
457 Population Growth and Land Use Exploitation in the Coastal Aquifers of Sri Lanka, Southern
458 Illinois University Carbondale 2008, 43.

459 Jayasekera, D. L., Kaluarachchi, J. J., and Villholth, K. G.: Groundwater stress and vulnerability
460 in rural coastal aquifers under competing demands: a case study from Sri Lanka, *Environ Monit*
461 *Assess.*, 176, 13-30, <https://doi.org/10.1007/s10661-010-1563-8>, 2011.

462 Kardan Moghaddam, H., Jafari, F., and Javadi, S.: Vulnerability evaluation of a coastal aquifer via
463 GALDIT model and comparison with DRASTIC index using quality parameters, *Hydro. Sci. J.*,
464 62, 137-146, <https://doi.org/10.1080/02626667.2015.1080827>, 2017.

465 Kumar, P., Thakur, P. K., Bansod, B. K., and Debnath, S. K.: Assessment of the effectiveness of
466 DRASTIC in predicting the vulnerability of groundwater to contamination: a case study from
467 Fatehgarh Sahib district in Punjab, India, *Environ. Earth. Sci.*, 75, 879,
468 <https://doi.org/10.1007/s12665-016-5712-4>, 2016.

469 Madrucci, V., Taioli, F., and de Araújo, C. C.: Groundwater favorability map using GIS
470 multicriteria data analysis on crystalline terrain, Sao Paulo State, Brazil, *J. Hydro.*, 357, 153-173,
471 <https://doi.org/10.1016/j.jhydrol.2008.03.026>, 2008.

472 Manap, M. A., Sulaiman, W. N. A., Ramli, M. F., Pradhan, B., and Surip, N.: A knowledge driven
473 GIS modeling technique for groundwater potential mapping at the Upper Langat Basin, Malaysia,
474 *Arabian. J. Geosci.*, 6, 1621-1637, <https://doi.org/10.1007/s12517-011-0469-2>, 2013.

475 Manap, M. A., Nampak, H., Pradhan, B., Lee, S., Sulaiman, W. N. A., and Ramli, M. F.:
476 Application of probabilistic-based frequency ratio model in groundwater potential mapping using
477 remote sensing data and GIS, *Arabian. J. Geosci.*, 7, 711-724, [https://doi.org/10.1007/s12517-](https://doi.org/10.1007/s12517-012-0795-z)
478 [012-0795-z](https://doi.org/10.1007/s12517-012-0795-z), 2014a.

479 Manap, M. A., Nampak, H., Pradhan, B., Lee, S., Sulaiman, W. N. A., and Ramli, M. F.:
480 Application of probabilistic-based frequency ratio model in groundwater potential mapping using
481 remote sensing data and GIS, *Arabian. J. Geosci.*, 7, 711-724, [https://doi.org/10.1007/s12517-](https://doi.org/10.1007/s12517-012-0795-z)
482 [012-0795-z](https://doi.org/10.1007/s12517-012-0795-z), 2014b.

483 Martínez-Bastida, J. J., Arauzo, M., and Valladolid, M.: Intrinsic and specific vulnerability of
484 groundwater in central Spain: the risk of nitrate pollution, *Hydro. J.*, 18, 681-698,
485 <https://doi.org/10.1007/s10040-009-0549-5>, 2010.

486 Merchant, J. W.: GIS-based groundwater pollution hazard assessment: a critical review of the
487 DRASTIC model, *Photogramm Eng Remote Sensing.*, 60, 1117-1127, 1994.

488 Modabberi, H., Hashemi, M. M. R., Ashournia, M., and Rahimpour, M. A.: Sensitivity Analysis
489 and Vulnerability Mapping of the Guilan Aquifer Using Drastic Method, *Rev. Environ. Earth. Sci.*,
490 4, 27-41, <https://doi.org/10.18488/journal.80.2017.41.27.41>, 2017.

491 Napolitano, P., and Fabbri, A.: Single-parameter sensitivity analysis for aquifer vulnerability
492 assessment using DRASTIC and SINTACS, Proceedings of the Vienna Conference, Netherlands,
493 1996, 559-566.

494 National Research Council: Ground water vulnerability assessment: Predicting relative
495 contamination potential under conditions of uncertainty. National Academies Press, USA, 224,
496 1993.

497 Neshat, A., Pradhan, B., Pirasteh, S., and Shafri, H. Z. M.: Estimating groundwater vulnerability
498 to pollution using a modified DRASTIC model in the Kerman agricultural area, Iran, Environ.
499 Earth. Sci., 71, 3119-3131, <https://doi.org/10.1007/s12665-013-2690-7>, 2014.

500 Neshat, A., and Pradhan, B.: Evaluation of groundwater vulnerability to pollution using DRASTIC
501 framework and GIS, Arabian. J. Geosci., 10, 2-8, <https://doi.org/10.1007/s12517-017-3292-6>,
502 2017.

503 Raju, N. J., Ram, P., and Gossel, W.: Evaluation of groundwater vulnerability in the lower Varuna
504 catchment area, Uttar Pradesh, India using AVI concept, J. Geol. Soc. India., 83, 273-278,
505 <https://doi.org/10.1007/s12594-014-0039-9>, 2014.

506 Saida, S., Tarik, H., Abdellah, A., Farid, H., and Hakim, B.: Assessment of groundwater
507 vulnerability to nitrate based on the optimised DRASTIC models in the GIS Environment (Case
508 of Sidi Rached Basin, Algeria), Geosciences, 7, 2-23,
509 <https://doi.org/10.3390/geosciences7020020>, 2017.

510 Saidi, S., Bouri, S., and Ben Dhia, H.: Sensitivity analysis in groundwater vulnerability assessment
511 based on GIS in the Mahdia-Ksour Essaf aquifer, Tunisia: a validation study, Hydro. Sci. J., 56,
512 288-304, <https://doi.org/10.1080/02626667.2011.552886>, 2011.

513 Samake, M., Tang, Z., Hlaing, W., Mbue, I. N., Kasereka, K., and Balogun, W. O.: Groundwater
514 vulnerability assessment in shallow aquifer in Linfen Basin, Shanxi Province, China using
515 DRASTIC model, *J. Sustain. Develop.*, 4, 53-71, <https://doi.org/10.5539/jsd.v4n1p53>, 2011.

516 Sarah, C., and Patricia I, C.: Ground water vulnerability assessment: Predicting relative
517 contamination potential under conditions of uncertainty, National Academies Press, USA, 1993.

518 Secunda, S., Collin, M., and Melloul, A. J.: Groundwater vulnerability assessment using a
519 composite model combining DRASTIC with extensive agricultural land use in Israel's Sharon
520 region, *J. Environ. Manage.*, 54, 39-57, <https://doi.org/10.1006/jema.1998.0221>, 1998.

521 Shirazi, S. M., Imran, H., and Akib, S.: GIS-based DRASTIC method for groundwater
522 vulnerability assessment: a review, *J. Risk. Res.*, 15, 991-1011,
523 <https://doi.org/10.1080/13669877.2012.686053>, 2012.

524 Singh, A., Srivastav, S., Kumar, S., and Chakrapani, G. J.: A modified-DRASTIC model
525 (DRASTICA) for assessment of groundwater vulnerability to pollution in an urbanized
526 environment in Lucknow, India, *Environ. Earth. Sci.*, 74, 5475-5490,
527 <https://doi.org/10.1007/s12665-015-4558-5>, 2015.

528 Souleymane, K., and Tang, Z.: A novel method of sensitivity analysis testing by applying the
529 DRASTIC and fuzzy optimization methods to assess groundwater vulnerability to pollution: the
530 case of the Senegal River basin in Mali, *Nat. Hazards. Earth. Sys. Sci.*, 17, 1375-1392,
531 <https://doi.org/10.5194/nhess-17-1375-2017>, 2017.

532 Srivastava, P. K., and Bhattacharya, A. K.: Groundwater assessment through an integrated
533 approach using remote sensing, GIS and resistivity techniques: a case study from a hard rock
534 terrain, *Int. J. Remote. Sens.*, 27, 4599-4620, <https://doi.org/10.1080/01431160600554983>, 2006.

535 Tilahun, K., and Merkel, B. J.: Assessment of groundwater vulnerability to pollution in Dire Dawa,
536 Ethiopia using DRASTIC, *Environ. Earth. Sci.*, 59, 1485-1496, <https://doi.org/10.1007/s12665>
537 009-0134-1, 2010.

538 Zghibi, A., Merzougui, A., Chenini, I., Ergaieg, K., Zouhri, L., and Tarhouni, J.: Groundwater
539 vulnerability analysis of Tunisian coastal aquifer: an application of DRASTIC index method in
540 GIS environment, *Groundwater. Sustain. Develop.*, 2, 169-181,
541 <https://doi.org/10.1016/j.gsd.2016.10.001>, 2016.

542